Saudi Pharmaceutical Journal 32 (2024) 102153

HOSTED BY

Contents lists available at ScienceDirect

Saudi Pharmaceutical Journal

journal homepage: www.sciencedirect.com

Enhanced anti-tumor therapy for hepatocellular carcinoma via sorafenib and KIAA1199-siRNA co-delivery liposomes

Yao Yao [a], Qian Zhao [b], Feng Xu [a,*], Tingting Yao [b,*]

[a] Guangdong Food and Drug Vocational College, Guangzhou, China
[b] Department of Gynecological Oncology, Sun Yat-Sen Memorial Hospital, Sun Yat-Sen University, Guangzhou, China

ARTICLE INFO

Keywords:
Sorafenib
siRNA
Co-loaded
Co-delivery
Hepatocellular carcinoma

ABSTRACT

Hepatocellular carcinoma (HCC) is one of the most lethal malignancies worldwide. Sorafenib (Sf) is currently the first-line treatment for HCC. However, due to the side effects and unsatisfied efficiency of Sf, it is urgent to combine different therapeutic agents to inhibit HCC progression and increase the therapeutic efficacy. Here, our study constructed a Sf and KIAA1199-siRNA co-loaded liposome Sf-Lp-KIAA, which was prepared by electrostatic interaction of KIAA1199-siRNA and Sf loaded liposome (Sf-Lp). The particle size, zeta potential, the in vitro cumulative release was investigated. The physical and chemical properties were characterized, and the inhibition of HepG2 growth and metastasis in vitro was investigated. The cellular uptake of the co-loaded liposome was significantly higher than that of free siRNA, and the drug/siRNA could be co-delivered to the target cells. Sf-Lp-KIAA could significantly inhibit the growth, migration, invasion and down-regulate KIAA1199 expression of HepG2 cells in vitro than that of single Sf treated group. In addition, the co-delivery liposome accumulated in the HepG2 subcutaneous tumor model and suppress tumor growth after systemic administration without induce obvious toxicity. The present study implied that the co-delivery of Sf and KIAA1199-siRNA through the co-loaded liposomes exerted synergistic antitumor effects on HCC, which would lay a foundation for HCC therapy in the future.

1. Introduction

As one of the common malignant tumors, hepatocellular carcinoma (HCC) has an insidious onset and poor prognosis. The high recurrence rate and metastasis rate have become the main problems affecting the clinical efficacy of HCC(Ahn et al., 2021). It is an urgent issue to explore suitable strategies to inhibit the growth and metastasis of tumor cells to improve the treatment effect of HCC. Sorafenib (Sf) is a first-line chemotherapy drug for the treatment of HCC worldwide. However, Sf is effective in only 30 % of HCC patients, inducing different adverse events such as high blood pressure, abdominal pain, gastrointestinal or skin diseases(Tang et al., 2020), patients who discontinue sorafenib may have tumor recurrence(Desar et al., 2009). The poor solubility and rapid clearance of Sf cause low distribution in tumor tissues(Gopakumar et al., 2022; Kong et al., 2021). On the other hand, it has been found that a certain dose of Sf can increase the invasion and metastasis of HCC {Jiang, 2018 #24}{Zhang, 2012 #23}.

Although many Sf monotherapies have been investigated to improve its solubility and antitumor efficacy, the clinical benefits did not show enough potential(Caputo et al., 2022; Chirayil & Kumar, 2022; Rimassa et al., 2023; C. Yang et al., 2023). Therefore, combined or multiple therapeutic strategies have been proposed as a promising therapeutic modality to enhance the anti-tumor ability of Sf as well as regulate the process of proliferation and migration of liver cancer cells (C. Jiang et al., 2018; X. Wang et al., 2022; C. Yang et al., 2023; You et al., 2016).

Currently, combination of antitumor agent with small interfering RNA (siRNA) has been considered as an alternative approach(Safaei et al., 2023). RNA interference (RNAi) therapy plays an essential role in

Abbreviations: **HCC**, hepatocellular carcinoma; **Sf**, sorafenib; **KIAA1199-siRNA**, a small interfering RNA that silences the KIAA1199 gene; **Sf-Lp-KIAA1199**, sorafenib and KIAA1199-siRNA co-loaded liposomes; **Sf-Lp**, sorafenib loaded liposomes; **Lp**, blank liposomes; **Sf-Lp-FAM**, sorafenib and FAM labeled siRNA co-loaded liposomes; **Sf-Lp-NC**, Sf and non-targeted control siRNA co-loaded liposomes; **Cou-Lp-Cy3**, Coumarin-6 and Cy3-siRNA co-loaded liposomes; **Dir-Lp-KIAA**, Dir and KIAA-siRNA co-loaded liposomes.

* Corresponding authors at: No.321 Longdong North Road, Tianhe District, Guangzhou 510520, China.(F. Xu) Department of Gynecological Oncology, Sun Yat-Sen Memorial Hospital, Sun Yat-Sen University, 107 Yan Jiang West Road, Guangzhou 510120, China (T. Yao).

E-mail addresses: xuf@gdyzy.edu.cn (F. Xu), yaotting@mail.sysu.edu.cn (T. Yao).

https://doi.org/10.1016/j.jsps.2024.102153
Received 27 December 2023; Accepted 26 July 2024
Available online 28 July 2024

tumor combination therapy owing to precise knockdown of oncogene through siRNA(Safaei et al., 2022), which consequently reduce systemic toxicity caused by chemotherapy drugs. KIAA1199, an important member of the KIAA gene family, is overexpressed in human liver cancer tissues and metastatic HCC cell lines(H. Kim et al., 2020; D. Wang et al., 2020). It has been reported that KIAA1199 regulates the progression of hepatocellular carcinoma by affecting the epithelial-mesenchymal transition process and is significantly associated with the five-year survival rate and prognosis of liver cancer patients (Z. Jiang et al., 2018). Henceforth, the combination of siRNA approach for targeting KIAA1199 gene with traditional chemotherapy drugs could be implemental for enhancing therapeutic efficiency of HCC.

Given that the physicochemical properties of siRNA and chemotherapeutic drugs are different, it is crucial to design one singular system capable of packing these two therapeutic agents and synchronously delivering drug/siRNA to the intended site. For example, PAMAM dendrimers were designed to co-encapsulate Bcl-2 siRNA and curcumin for cervical cancer treatment(Ghaffari et al., 2020). A Hela cancer cell membrane-biomimetic PLGA-based nanocarrier was designed to co-deliver PTX and siRNA targeting HPV18-E7(C. Xu et al., 2020). Carboxymethyl chitosan-modified liposomes were prepared for co-delivery of Sf and Cy3-siRNA(Yao et al., 2015).To date, liposomes have gradually become a representative nanocarrier for combined or multiple therapies due to their low toxicity, simple preparation process, and the ability to simultaneously encapsulate drugs of different properties(Eftekhari et al., 2019; Ye et al., 2021). In this study, a Sf and KIAA1199-siRNA co-loaded liposome Sf-Lp-KIAA1199 was developed, motivating by the hypothesis that KIAA1199-siRNA could improve the therapeutic effect of Sf and co-delivery of two antitumor agents would exert synergetic antitumor effects. The physicochemical properties, the in vitro and in vivo antitumor ability of Sf-Lp-KIAA1199 were investigated, which would provide an alternative idea for the treatment of HCC.

2. Material and methods

2.1. Materials

Sorafenib was purchased from Solarbio Life Sciences (Beijing, China); egg phospholipid PC-98 T was purchased from AVT Pharmaceutical Co., Ltd. (Shanghai, China); (2,3-Dioleoyloxy-propyl)-trimethylammonium-chloride (DOTAP), N-(carbonyl-methoxypolyethyleneglycol-2000)-1,2-distearoyl-*sn*-glycero-3-phosphothanolamine (DSPE-PEG2000) were purchased from Avanti Polar Lipids (Alabaster, USA); Cholesterol was purchased from Solarbio Life Sciences (Beijing, China); KIAA1199-siRNA, FAM labeled non-sense siRNA (FAM-siRNA), Cy3 labeled non-sense siRNA (Cy3-siRNA), Non-targeted control siRNA (NC-siRNA) were synthesized by RiboBio Co., Ltd. (Guangzhou, China); Agarose was purchased from Aladdin Co., Ltd. (Beijing, China); CCK-8 kits were purchased from Beyotime Biotechnology Co., Ltd. (Shanghai, China); Transwell chambers and BioCoatTM matrix invasion chambers were purchased from Corning Life Sciences(NY, USA); KIAA1199 antibody was obtained from Biotech Co., Ltd. (Beijing, China); HRP conjugated secondary antibody was obtained from Boster Biological Technology Co., Ltd. (Wuhan, China); HRP labeled GAPDH antibody was purchased from Kangcheng Biological Engineering Co., Ltd. (Shanghai, China); The PVDF membrane was purchased from Millipore (Billerica, USA); All other chemical reagents were of analytic grade or above.

The HepG2 cells were obtained from Shanghai Cell Bank and cultured in RPMI 1640 medium with 10 % fetal bovine serum. BALB/c nude mice (Male, 4–6 weeks old, 16–20 g) were purchased from Guangzhou Ruige Biological Technology Co., LTD (Guangzhou, China). All the animal experiments were performed in accordance with the Guide for the Care and Use of Laboratory Animals.

2.2. Preparation of Sf and KIAA1199-siRNA co-loaded liposomes

Liposome was prepared by thin film dispersion-extrusion method. In brief, DOTAP, PC-98 T, cholesterol, DSPE-PEG2000 and Sf (5:9:4.5:0.9:1, mol/mol) were dissolved in ethanol at 45℃. A lipid film was formed after rotary evaporation and then was hydrated with 5 % glucose for 20 min at 40℃. Subsequently, the Sf loaded liposomes (Sf-Lp) were obtained by extruding through 400 and 200 nm polycarbonate membranes using a LF-1 Mini liposome extruder (Ottawa, Canada). The blank liposomes (Lp) were prepared by the same method above. Then, the Sf-Lp and KIAA1199-siRNA solution were mixed in a certain proportion and incubated for 10 min to obtain Sf and KIAA1199-siRNA co-loaded liposomes (Sf-Lp-KIAA). The preparation process of Sf and non-targeted control siRNA co-loaded liposomes (Sf-Lp-NC) was similar with that of Sf-Lp-KIAA.

2.3. Particle size and zeta potential

The particle size distribution and zeta potential of liposomes were measured by a dynamic light scattering method using the Malvern Zetasizer Nano ZS (Malvern, UK). The samples were diluted to 10 μg/mL lipid concentration with double distilled water and placed in the sample pool. Measurements were tested at a 90° angle at 25℃.

2.4. Morphology

Sf-Lp or Sf-Lp-KIAA diluted with distilled water was placed in a copper grid, dried and stained with 2 % phosphor tungstic acid. The excess liquid was absorbed by filter paper and the sample was observed under a JEM-2010HR high-resolution transmission electron microscope (Tokyo, Japan).

2.5. Agarose gel electrophoresis

The siRNA binding ability was performed by gel retardation assay. The 2 % agarose gel containing 0.1 μL /mL Goldview was prepared, and Sf-Lp-KIAA at different weight ratios of DOTAP and siRNA was loaded into individual gel wells for electrophoresis with a voltage of 90 V for 15 min. After electrophoresis the gel images were photographed through a gel imaging system (Liuyi Biotechnology, Beijing, China).

2.6. Loading efficiency

To measure the encapsulation efficiency of Sf in the liposomes, 0.1 mL Sf-Lp was dispersed in 0.4 % Tween 80-PBS solution and centrifuged for 30 min at a rotating speed of 16,000 r/min. Then the supernatant was transferred to a 10 mL volumetric bottle with ethanol to determine the amount of free Sf in the supernatant by HPLC(Yao et al., 2015). An appropriate amount of Sf-Lp was taken into a 10 mL volumetric bottle and demulsified with ethanol. The total amount of the drug was determined by HPLC. The encapsulation efficiency (EE) and drug loading (DL) of Sf were calculated according to the following formula.

$$EE(\%) = \frac{\mathrm{Wt} - \mathrm{W}}{Wt} \times 100\%$$

$$DL(\%) = \frac{\mathrm{Wd}}{\mathrm{W0}} \times 100\%$$

Where Wt is the total amount of Sf, W is the weight of Sf in the supernatant, Wd is the weight of encapsulated Sf and W0 is the total amount of Sf and lipids.

2.7. In vitro release

The in vitro release of Sf from Sf-Lp-KIAA was investigated by dynamic dialysis method. A volume of 2 mL Sf-Lp-KIAA in a dialysis bag

(molecular weight: 8000–14000 Da) was immersed into 13 mL PBS containing 1 % (w/v) Tween 80 and constant oscillated (100 rpm/min) at 37 ℃for 48 h. 2 mL sample was taken out at 0.5, 1, 2, 4, 8, 12, 24 and 48 h, respectively, and an equal amount of isothermal release medium was added after each sampling. The concentration of Sf in samples were determined by HPLC at the detection wavelength of 265 nm.

2.8. Cellular uptake

To investigate the cellular uptake by HepG2 cells, FAM-siRNA was used to prepare co-loaded liposome Sf-Lp-FAM. The HepG2 cells were seeded in a 12-well plate at the density of 10^4 cells per well and cultured at 37 ℃ overnight. After that, the original medium was removed and the cells were gently rinsed with PBS three times, then the free FAM-siRNA or Sf-Lp-FAM diluted with serum free RPMI-1640 culture medium was added into the corresponding wells respectively. The final concentration of FAM-siRNA in each well is 20 nM. At the end of 4 h incubation, the cells were washed three times with PBS, and photographed with inverted fluorescent microscope (Nikon, TE2000E, Tokyo, Japan). Then the cells were digested and collected with trypsin, and FAM positive cells were detected by a flow cytometry (BD, Franklin Lakes, USA).

2.9. Cellular co-delivery

Coumarin-6 and Cy3-siRNA was incorporated to prepare co-loaded liposome Cou-Lp-Cy3 to evaluate the cellular co-delivery. HepG2 cells were placed in 12-well plates at a density of 5×10^4 per well and cultured at 37℃. The Cou-Lp-Cy3 was diluted in the medium of serum-free RPMI-1640 and then added into corresponding wells. The final concentration of Cy3-siRNA and Coumarin 6 was 20 nM and 0.4 μM, respectively. After that, the cells were washed with cold PBS solution for three times and fixed with 4 % paraformaldehyde for 15 min. Then 5 μg/mL DAPI solution was added to stain nucleus and incubated at 37℃ for 10 min. The cellular co-delivery was observed and photographed under an inverted fluorescence microscope.

2.10. In vitro cytotoxicity

Cytotoxicity was detected by Cell Counting Kit-8 (CCK-8) assays. HepG2 cells were cultured in 96-well plates with a density of 4×10^3 per well and then replaced with serum-free medium. Free Sf was dissolved in Tween 80-ethanol (1:1, v/v). Different groups were diluted to a certain concentration with serum-free medium and added into 96-well plates, in which the final concentration of Sf was 1–32 μM and the final concentration of KIAA1199-siRNA was 50 nM. After incubation for 48h, the CCK-8 was added to each well and incubated for 1 h. After the treatment period, the absorbance was measured at 450 nm using an enzyme marker to calculate the cell survival rate.

2.11. Cell migration and invasion assays

To evaluate cell migration and invasion, HepG2 cells were seed in 12-well plates with a density of 5×10^4 per well, and then replaced with serum-free medium. Free Sf or Sf-contained liposomes were added into each well, where the Sf concentration was 8 μM and the KIAA1199-siRNA concentration was 50 nM, respectively. After incubation for 6 h, the serum medium was replaced with complete medium and the cells were continuously cultured for 42 h. The cells were harvested and added into the upper transwell chamber with the non-coated matrigel membrane (for migration assay) or with coated by matrigel (Corning Life Sciences, Corning, USA) for invasion assay. After incubation for another 24 h, the transwell chambers were washed with PBS solution, the migrated or invaded cells on the upper side of chambers were fixed with 90 % ethanol and stained in 0.1 % crystal violet, then photographed by an optical microscope and were quantified in five independent fields in each sample. The experiments were repeated three times and the data are showed as the means ± SD.

2.12. Real-time qPCR

RNA was extracted from the cells using a Total RNA Extraction Kit (Promega, Shanghai, China) and reverse-transcribed using a first-strand-cDNA synthesis kit (Thermo, Beijing, China). PCR was performed using SYBR Green/ROX qPCR Master Mix (Thermo, Beijing, China) and quantitatively assessed on a Step One real-time PCR system (Applied Biosystems, CA, USA). Gene expression level was normalized to GAPDH mRNA using the 2–ΔΔCT method. The primer sequences in the Real time-qPCR for GAPDH and KIAA1199 were 5′-ACTCCTCCACCTTTGACGCT-3′(GAPDH-forward), 5′-GGTCTCTCTCTTCCTCTTGTGC-3′(GAPDH-reverse), 5′-GATGTGCTCGTACTCCCTCG-3′(KIAA1199-forward) and 5′-CGGTTGTTGAGGCAATGTGG-3′(KIAA1199-reverse), respectively.

2.13. Western blot analysis

The cells were lysed in RIPA buffer on ice, total proteins were extracted from the cells and the total protein concentration was determined by BCA protein assay Kit. 40 μg of proteins were separated by 8–10 % SDS-PAGE (Bio-rad, Hercules, CA) and transferred to PVDF membranes (Millipore, Bedford, USA), then PVDF membranes were blocked with 5 % bovine serum albumin (BSA) and subsequently incubated with primary antibodies anti-KIAA1199 (1:500 dilution) overnight at 4 °C, GAPDH (1:5000 dilution) was detected as an internal control. Afterwards, the PVDF membranes were then washed in TBST (0.02 M TBS with 0.1 % Tween-20) three times and then incubated with HRP-conjugated goat anti-rabbit secondary antibody (1:5000 dilution) for 1 h, the protein blot was exposed by using the enhanced chemiluminescence (ECL) reagents (Applygen, Beijing, China). Image J software was used to analyze the gray value of the blot.

2.14. Animal models

The xenograft tumor models were established by subcutaneously inoculation of 0.1 mL HepG2 cell suspension (1×10^7 cells) into the right flank of the mice. The width and length of the tumor was measured by the caliper and the tumor volumes were calculated by the formula: $V=L\times W^2/2$, where L is the longest diameter and W is the shortest diameter perpendicular to length.

2.15. In vivo real-time fluorescence imaging

When the tumors reached to 200 mm^3, the HepG2 tumor-bearing nude mice were intravenously administrated by the free near-infrared dye Dir and Dir/KIAA-siRNA co-loaded liposomes (Dir-Lp-KIAA) at the Dir dose of 0.2 mg/kg. The in vivo imaging system (BLT AniView100, Guangzhou, China) was used to monitor the Dir fluorescence signal at different time intervals. After 24 h of administration, the mice were sacrificed to collect the tumor and the major tissues (heart, liver, spleen, lung, kidney) for imaging under the live imaging system.

2.16. In vivo antitumor efficacy

After the tumor reached to approximately 80–130 mm^3, the HepG2 tumor-bearing mice were divided into 6 groups randomly (n = 3) and were intravenously administrated by different preparations: 5 % glucose solution (control group), free Sf (7 mg Sf/kg), Sf-Lp (7 mg Sf/kg), Sf-Lp-NC (7 mg Sf/kg and 1.0 mg NC-siRNA/kg), Sf-Lp-KIAA (7 mg Sf/kg and 1.0 mg KIAA-siRNA/kg) and blank Lp group every two days for six times. During the period, the tumor sizes and body weights were measured every other day. At the end of the treatment, the mice were euthanized, the harvested tumors were weighted and photographed. Then the tumors and main organs were collected and fixed by 4 %

paraformaldehyde for further studies.

2.17. H&E and TUNEL assay

The hematoxylin and eosin (H&E) staining was used to evaluate the pathological changes in tumor tissues. Additionally, the TUNEL staining was used to detect the tumor cell apoptosis. Briefly, the fixed tumors were paraffin embedded, sectioned, deparaffinized and subjected to H&E staining assay or TUNEL assay kit instructions. The major organs including heart, liver, spleen, lungs, and kidneys were also treated with H&E staining to assess the organ-specific toxicity. The sections were deparaffinized, stained by immunohistochemistry test and observed under an optical microscope (Eclipse Ts2, Nikon, China).

2.18. Statistical analysis

The data are presented as the means ± standard deviations (SD) from at least three repeated experiments. Inter-group differences were tested using one-way analysis of variance (ANOVA). $P<0.05$ was considered statistically significant ('*' as presented), $P<0.01$ was considered extremely statistically significant ('**' as presented).

3. Results

3.1. Preparation and characterization of Sf-Lp-KIAA

The Sf-Lp morphology was observed by transmission electron microscopy (TEM), which was spherical and rounded in shape (Fig. 1A). The average particle size measured by laser particle analyzer was (182.5 ± 6.1) nm with the PDI of 0.153 ± 0.012, and the zeta potential was (39.7 ± 2.2) mV (Fig. 1B.C). The encapsulation efficiency was (88.2 ± 2.6) %, and the Sf loading was (5.1 ± 0.1) %.

Upon Sf-Lp and KIAA1199-siRNA mixing at room temperature, electrostatic interactions led to co-loaded liposomes (Sf-Lp-KIAA) formation over a range of DOTAP/ KIAA1199-siRNA mass ratios from 20:1 to 200:1. Agarose gel electrophoresis was used to perform the most suitable combination of Sf-Lp and siRNA, with free siRNA as the control. Meanwhile, the particle size and zeta potential of Sf-Lp-KIAA with different mass ratios were determined. The results of agarose gel electrophoresis (Fig. 1G) showed that the free siRNA migrated with electrophoresis and appeared bright bands. After the addition of Sf-Lp, the siRNA bands became shallow, and when the DOTAP/siRNA mass ratio reached 80:1, the siRNA bands disappeared completely. According to the results of particle size and zeta potential measurement (Fig. 1H.I), when the mass ratio of DOTAP to siRNA increased, the particle size reduced and the zeta potential reversed from negative to positive. When the mass ratio reached 80:1, the particle size tended to stable and the

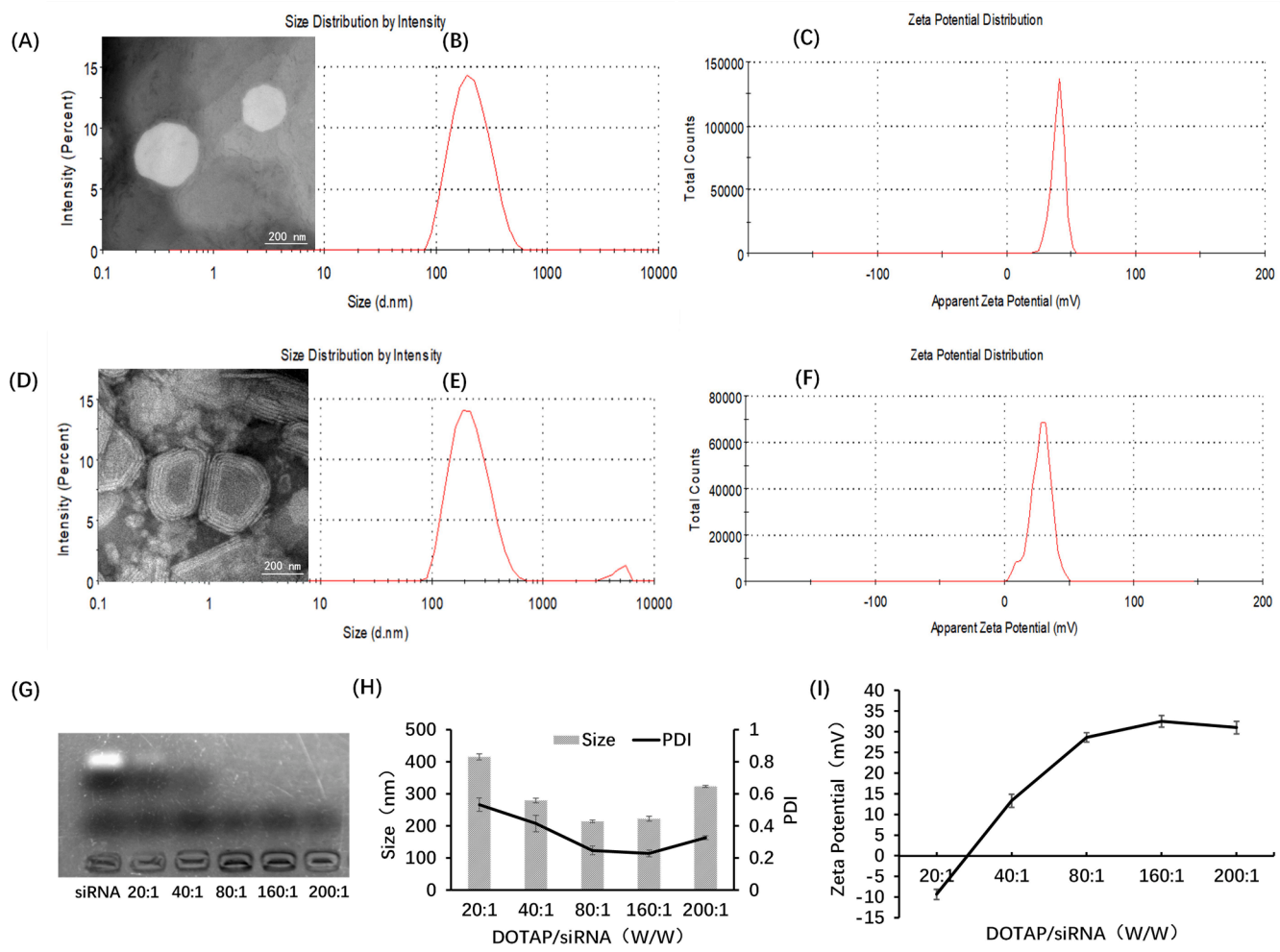

Fig. 1. Characterization of sorafenib single-loaded liposomes (Sf-Lp) and co-loaded liposomes (Sf-Lp-KIAA). A, Transmission electron microscopy (TEM) image of Sf-Lp. B, C, Particle size and zeta potential distributions of Sf-Lp. D, TEM image of Sf-Lp-KIAA. E, F, Size distribution and zeta potential of Sf-Lp-KIAA. G, Agarose gel electrophoresis of Sf-Lp-KIAA at varying DOTAP/siRNA mass ratios. H, Particle size and PDI of Sf-Lp-KIAA at varying DOTAP/siRNA mass ratios. I, Zeta potential of Sf-Lp-KIAA at varying DOTAP/siRNA mass ratios. Scale bar, 200 nm.

change of potential tends to be gentle. When the mass ratio exceeded 160:1, the particle size increased further, indicating that the optimal ratio was 80:1. Under these conditions, the mean particle size of Sf-Lp-KIAA is (214.07 ± 4.04) nm, the PDI is 0.247 ± 0.027, and the zeta potential is (28.6 ± 1.1) mV (Fig. 1E.F). The morphology observed by transmission electron microscopy showed the multilayer structure of lipoplex which formed by the compression of siRNA(Koide et al., 2016) (Fig. 1D). The cumulative release of Sf from Sf-Lp-KIAA and free drug solution was studied in PBS-Tween media at 37 ℃. As shown in Fig. 2, free Sf were released from Sf solution reached 55.0 % during the first 6 h and approximately 85 % was tested at 12 h. Compared with the rapid release of Sf solution, Sf-Lp-KIAA showed significant slower release behavior without initial bursts and 61 % of Sf released from the nanoparticulate system at the end of study period. The sustained release time coupled with the absence of burst release could minimize adverse effects in systemic treatments.

3.2. In vitro cellular uptake and co-delivery experiments

To investigate the cellular uptake of Sf-Lp-KIAA qualitatively and quantitatively, the fluorescent labeled FAM-siRNA was substituted for KIAA1199-siRNA to prepare the co-loaded liposome Sf-Lp-FAM. After incubation with HepG2 cells for 4 h, the fluorescence microscope was employed to observe the cellular internalization. Fig. 3A showed that the free siRNA group exhibited almost invisible fluorescence, whereas more obvious green fluorescence could be observed in the Sf-Lp-FAM group, indicating that the free siRNA was difficult to enter cells due to medium molecular weight and negative-charge density(Yonezawa et al., 2020), and the positively charged liposomes could improve the siRNA cell uptake, which was consistent with the corresponding flow cytometry analysis results. As shown in Fig. 3B, the positive rate of FAM in the free siRNA group was only about 1.2 %, while the positive rate of FAM in the Sf-Lp-FAM group was significantly higher ($P<0.01$).

The advantage of co-loaded carriers is to co-deliver drugs with different properties to the same target to create synergies(Eftekhari et al., 2019). In order to study the co-delivery ability of the co-loaded liposomes, Cy3-siRNA was substituted for KIAA1199-siRNA and coumarin-6 was substituted for Sf to obtain co-loaded liposome Cou-Lp-Cy3 with double fluorescence labeling. In Fig. 4, the red fluorescence was Cy3-siRNA, the green fluorescence was coumarin-6, blue fluorescence was the cell nucleus stained by DAPI, and yellow fluorescence in the merged view represented the co-localization of red fluorescence (Cy3-siRNA) and green fluorescence (coumarin-6). The results showed that Cy3-siRNA and coumarin-6 have entered in the cells at 1 h incubation time, and the yellow spots appeared in the overlaps. After 4 h, the red fluorescence and the green fluorescence signals were enhanced in respective panels, the yellow fluorescence area in the merged image was also increased, indicating that the co-loaded liposomes could co-deliver siRNA and drugs to the same cell, and the delivery ability would increase with time.

3.3. In vitro cytotoxicity

The cytotoxicity of different groups incubated with HepG2 cells for 48 h was investigated by CCK-8 method. As shown in Fig. 5, the blank liposomes exhibited approximately 25 %-31 % toxicity only between the high concentration of 16 μM and 32 μM (equal to Sf dose), which was attributed to the positive charge of the liposomes. The other groups exhibited a dose-dependent cytotoxicity. The half maximal inhibitory concentration (IC50) value of free Sf, Sf-Lp, Sf-Lp-NC and Sf-Lp-KIAA was 11.22, 23.50, 28.19, 14.74 μM, respectively. The cell viability and IC50 of Sf-Lp-NC was slightly higher than that of Sf-Lp owing to its relative lower surface charge. Furthermore, IC50 of Sf-Lp-KIAA was obviously lower in contrast to that of Sf-Lp and Sf-Lp-NC, implying that silencing the KIAA1199 expression could enhance the tumor inhibition of Sf in vitro and nonsense-sequence siRNA had no significant effect on proliferation inhibition. Additionally, though free Sf formulation showed higher cytotoxicity against cells at the concentration from 16 to 32 μM and the lowest IC50, it was not suitable for systemic administration because of its organic solvent.

3.4. Cell migration and invasion assays

To explore the impact of co-loaded liposomes on HCC metastasis in vitro, transwell models with or without Matrigel were used to detect the effects of Sf-Lp-KIAA on cell migration and invasion, respectively. As illustrated in the cell migration results (Fig. 6A), after 48 h incubation, the invasion abilities of Sf solution, Sf-Lp and Sf-Lp-NC treated cells was stronger than that of the control or Lp group, whereas the invading cells in the Sf-Lp-KIAA treatment group was significantly less than that in other groups. Similar to the invasion assay, more migrating cells were observed in the Sf solution group and Sf-Lp group, and the Sf-Lp-KIAA largely inhibited cell migration compared to other groups (Fig. 6B). Collectively, these results suggested that the single-Sf use might promote the invasion and migration of HepG2 cells, while combination of Sf and KIAA-siRNA would attenuate these effects.

3.5. Assessment of KIAA1199 mRNA and protein levels

The expression of KIAA1199 in cells was investigated by RT-qPCR and Western Blot assay, and the results were shown in Fig. 7A and B. Blank Lp had little silencing ability. The KIAA1199 mRNA level in free Sf treated group, Sf-Lp group and scrambled siRNA loaded Sf-Lp-NC group was similar ($P>0.05$), while the Sf-Lp-KIAA group showed remarkably decreased level compared to other groups. The Western Blot result also indicated that Sf-Lp-KIAA the co-loaded liposome Sf-Lp-KIAA could effectively inhibit the expression of KIAA1199 protein.

3.6. In vivo distribution of Sf-Lp-KIAA

The accumulation in tumor sites of the co-loaded liposomes were

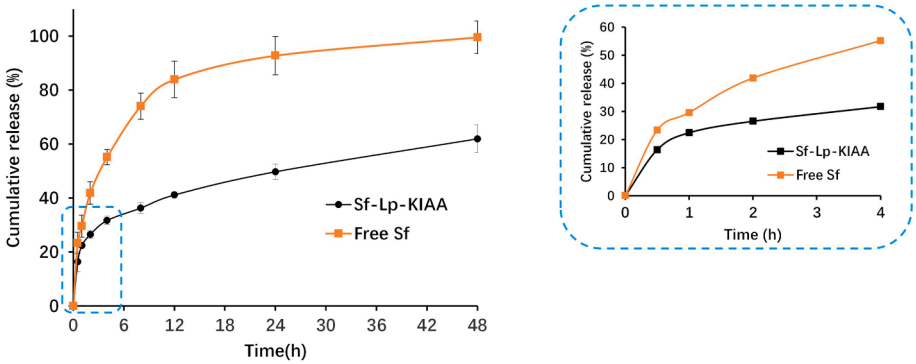

Fig. 2. Sf release profiles from Sf solution or Sf-Lp-KIAA in vitro. (means ± SD, n = 3).

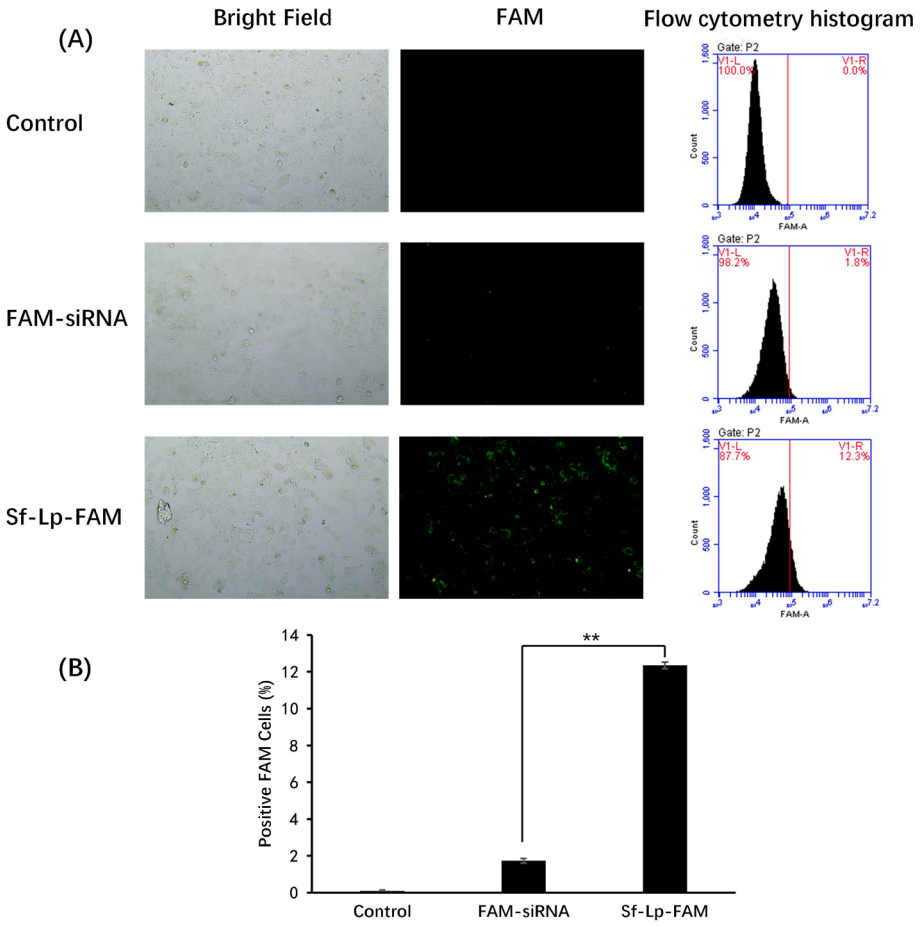

Fig. 3. Uptake characteristics of FAM-siRNA or sorafenib and FAM-siRNA co-loaded liposomes (Sf-Lp-FAM) in HepG2 cells. A, Fluorescence microscopy images and flow cytometric analysis of cellular uptake in cells. B, Quantitative analysis of the cellular uptake (means ± SD, n = 3, **p < 0.01).

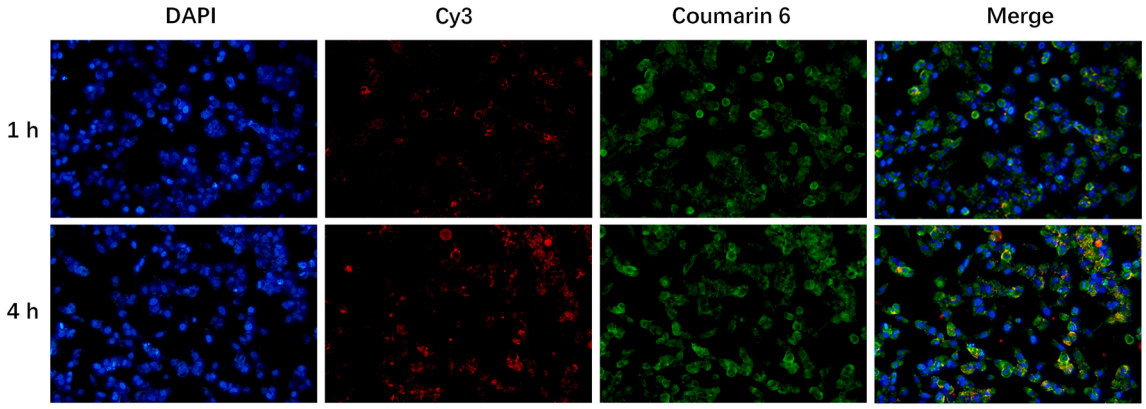

Fig. 4. Fluorescence microscopy images of HepG2 cells after incubated with Coumarin-6 and Cy3-siRNA co-loaded liposomes (Cou-Lp-Cy3) for 1 h and 4 h.

investigated by intravenously injecting the fluorescence probe Dir and KIAA-siRNA co-loaded liposomes (Dir-Lip-KIAA) into tumor-bearing mice at the Dir dosage of 2 mg/kg, free Dir was given as the positive control. As Fig. 8A exhibits, no obvious signal was detected at the tumor site in free Dir group during 24 h, while the Dir-Lp-KIAA group showed an enhanced signal in the tumor from 6 h to 24 h. At 24 h post-injection, tumor tissues and major organs were excised for further imaging. Fig. 8B and C showed that the Dir-Lp-KIAA displayed an evident tumor accumulation compared with free Dir at the 24 h time point, which was consist with the living image result.

3.7. In vivo antitumor efficiency and systemic toxicity

The antitumor efficiency and systemic toxicity of different formulations were evaluated in HepG2 subcutaneous xenograft mice. As shown in Fig. 9A, tumor volume of all groups exhibited varying degrees of growth. The tumor volume inhibiting rates of Sf solution, Sf-Lp, Sf-Lp-NC and Sf-Lp-KIAA were 16.36 %, 21.56 %, 29.93 % and 52.06 %, respectively, while the blank liposome alone could not inhibit tumor growth, exhibiting synergistic inhibitory effects of Sf and KIAA1199-siRNA. The result was confirmed by detecting the weight of isolated tumor tissues at the end of treatment, tumor weight of the Sf-Lp-KIAA

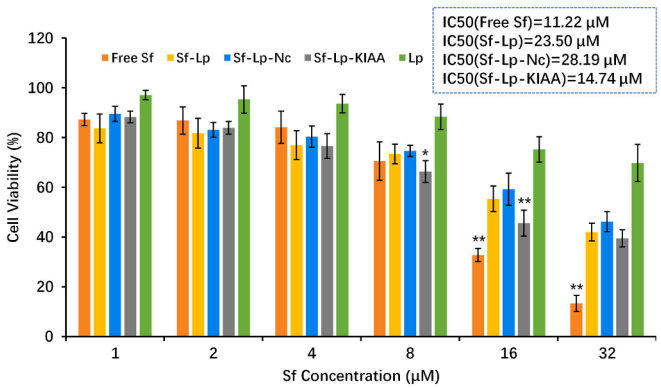

Fig. 5. Cytotoxicity on HepG2 cells after treated with Sf solution, Sf-Lp, Sf and nonsense-siRNA co-loaded liposomes (Sf-Lp-NC), Sf-Lp-KIAA, blank liposomes (Lp) for 48 h (means ± SD, n = 3, *P<0.05, **P<0.01).

group was the lowest among all the treatment groups (P<0.01, Fig. 9B). Body weights of mice in all groups did not show significant loss (Fig. 9C), illustrating the satisfactory biocompatibility of the co-loaded liposomes. The H&E staining results of heart, liver, spleen, lung and kidney were shown in Fig. 10. No significant pathological changes were observed in major organs compared with control group. H&E staining and TUNEL staining of tumor sections showed that the Sf-Lp-KIAA markedly decreased the number of tumor cells and effectively enhanced tumor apoptosis compared to those in other groups (Fig. 10).

4. Discussion

The mechanism of tumor occurrence and development is extremely complex, making it difficult to achieve effective treatment through monotherapy(Woodcock et al., 2011). Therefore, current strategies have focus on assembling different formulations into a single nanocarrier in order to generate an enhanced synergistic effect that overcomes the impediments of monotherapy. In this study, positively charged liposomes were prepared to co-load Sf and KIAA1199-targeted siRNA. The hydrophobic Sf was encapsulated in the phospholipid bilayer, and the cationic lipid DOTAP in the lipid membrane could efficiently compress hydrophilic siRNA to achieve drug and gene co-loading at the optimal potential.

An ideal drug/siRNA co-loaded delivery nanocarrier should reach and accumulate in tumor site, internalize into tumor cells and successfully release different therapeutic agents into the same cells to fully exert synergistic effects(Liu et al., 2019; Yi et al., 2022). This study verified that the co-loaded liposomes could overcome the membrane barrier, enter into cells and co-deliver Sf and siRNA into the same target cell. The co-delivery liposomes Sf-Lp-KIAA was subsequently revealed to lead to a great cytotoxicity and gene-silencing in HepG2 cells. Besides, the cell survival rate of all groups was above 70 % under the final concentration that Sf was 8 μM and KIAA1199-siRNA was 50 nM, ensuring that the liposomes can be transfected without causing obvious cytotoxicity in following cell experiments.

The motility and invasion of tumor cells is highly related to tumor progression. Despite the primary tumor growth inhibition effect, some evidence indicated that chemotherapeutic drugs could initiate metastasis(Li et al., 2022; Su et al., 2023). As the first-line chemotherapy drug for the treatment of HCC worldwide, Sf therapy has been reported inducing cell invasion and migration through modulated the EGF-induced epithelial-mesenchymal transition (EMT) by KIAA1199(Z. Jiang et al., 2018). In this study, though free Sf and Sf-Lp could inhibit HepG2 cells growth in vitro, these Sf single formulation induced significant migration or invasion compared with the untreated control group, which was in agreement with other studies(H. Wang et al., 2014; J. Xu et al., 2017; Y. Xu et al., 2019). What's more, although drug-free nanoparticulates may limit cell motion range and inhibit tumor cell removal (Cheng et al., 2022), the negligible invasion or migration in Lp treated group illustrated that the blank liposome had no effect on cell

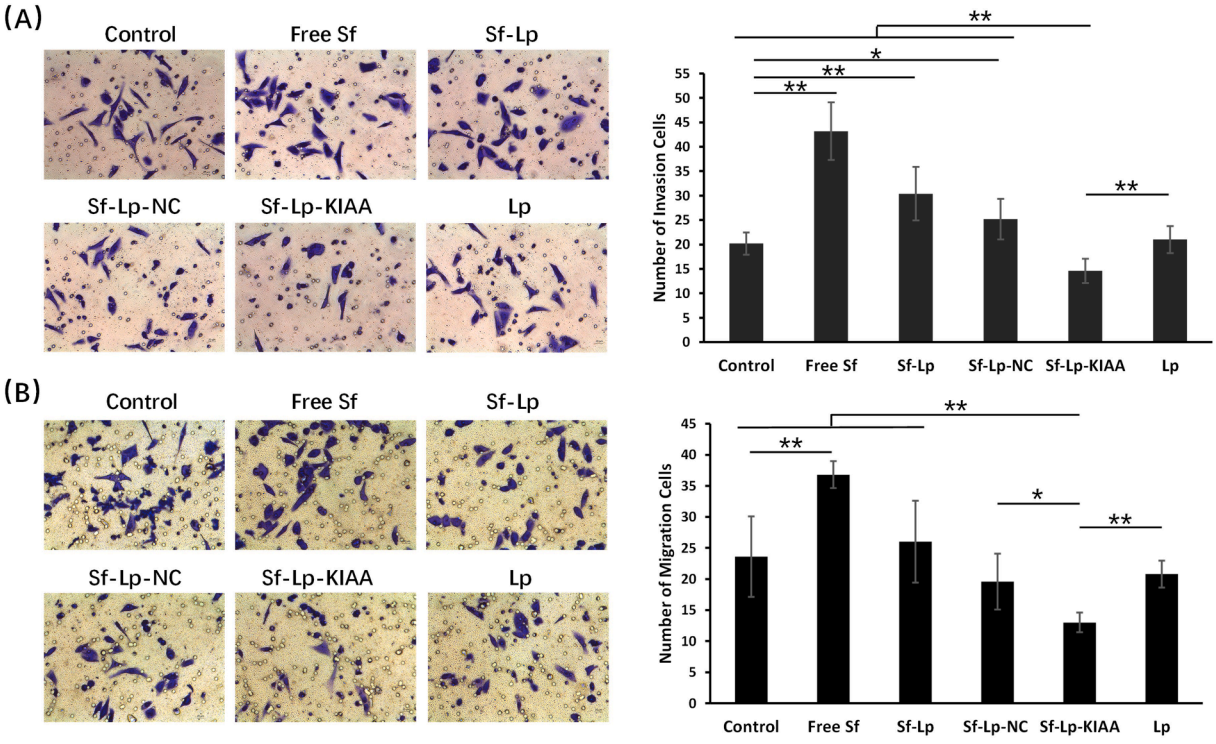

Fig. 6. In vitro inhibition of cell migration and invasion. A, Representative images (Scale bar: 100 μm) and invasion rate of HepG2 cells after treated with different formulations for 48 h. B, Representative images (Scale bar: 100 μm) and migration rate of HepG2 cells after treated with different formulations for 48 h (means ± SD, n = 3, *P<0.05, **P<0.01).

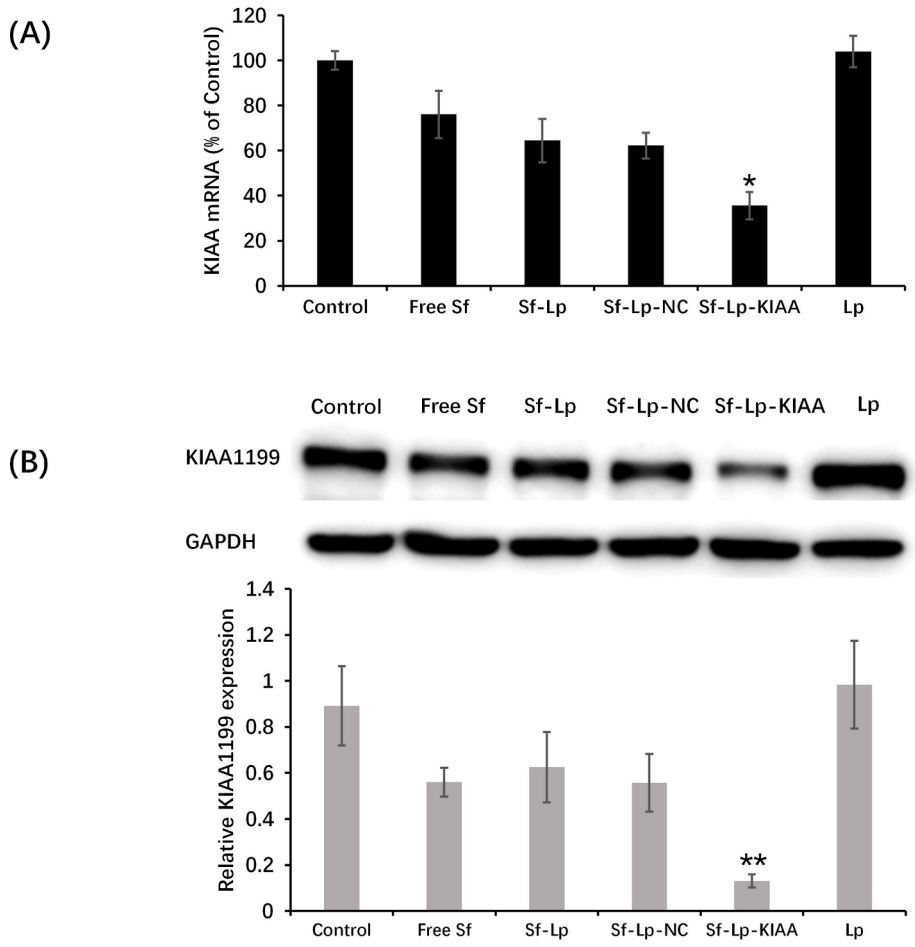

Fig. 7. Real-time qPCR and Western Blot assay of the expression of KIAA1199 in HepG2 cells after treatment with different formulations. A, The expression of KIAA1199 mRNA after different treatments by real-time qPCR (means ± SD, n = 3, *P<0.05). B, The expression of KIAA1199 after different treatments by WB(means ± SD, n = 3, *P<0.01). The full-length blots were included in the Supplementary Information.

invasion or migration. The PCR and Western Blot results suggested co-delivery of KIAA1199-siRNA with Sf could inhibit the invasiveness and metastatic potential in hepatocarcinoma in vitro model.

The in vivo distribution experiments exhibited that the co-loaded liposomes accumulated in tumor tissue after 24 h tail intravenous injection, it was mainly due to the EPR effect of PEGylated nanocarriers, which was a prerequisite for internalization and co-delivery of the co-loaded liposomes into the tumor cells. In addition, the liposomes showed higher uptake in liver, which was predominantly owing to the fact that liver macrophages or the abundant blood vessel could promote uptake and retention of 100–200 nm cationic liposomes in livers(J. Y. Kim et al., 2012; T. Yang et al., 2014). Furthermore, this phenomenon remind that the co-delivery liposomes may be suitable for the HCC therapy and research. Regarding to the in vivo antitumor experiment, the Sf solution just exhibited a mild antitumor effect, which did not completely correspond to the result of CCK-8 experiment. It mainly due to the cytotoxicity of the solvent (Tween 80-ethanol). The in vivo antitumor data demonstrated that Sf-Lp-KIAA showed the highest therapeutic effect as compared with control group and Sf formulation alone, suggesting that KIAA1199 was an effective therapeutic target for HCC treatment that could improve the therapeutic effect of Sf through the co-delivery liposome. In summary, we successfully prepared a Sf and KIAA1199-siRNA co-loaded liposome as a co-delivery platform in order to synergetic inhibit HCC. The liposome was able to co-deliver Sf and KIAA1199-siRNA to HepG2 cells, suppress cell proliferation, mitigate Sf-induced metastasis in vitro, and block tumor growth in vivo without obvious adverse side effects. which may serve as a potential strategy for the treatment of HCC. Our further study will focus on the inhibition of growth and metastasis on a HCC orthotopic tumor model by the co-delivery liposomes. Further efforts to confirm the antitumor effect of this delivery system in vivo will be warranted in our future study.

5. Funding Information

This work was financially supported by the Guangdong Province Natural Scientific Grant(2021A1515010267), the Basic and Applied Research Program of Guangzhou (202102021294),the Science and Technology Program General Project of Guangzhou(202201010782), the Medical Research Program of Guangdong Province (A2022160), the Traditional Chinese Medicine Bureau Program of Guangdong Province (20211283), the Guangdong Food and Drug Vocational College Research Fund (2017ZR004, 2018ZR017) and Csco-Pilot Cancer Research Fund (Y-2019AZMS-0393).

CRediT authorship contribution statement

Yao Yao: Writing – review & editing, Writing – original draft, Funding acquisition. **Qian Zhao:** Writing – review & editing, Software,

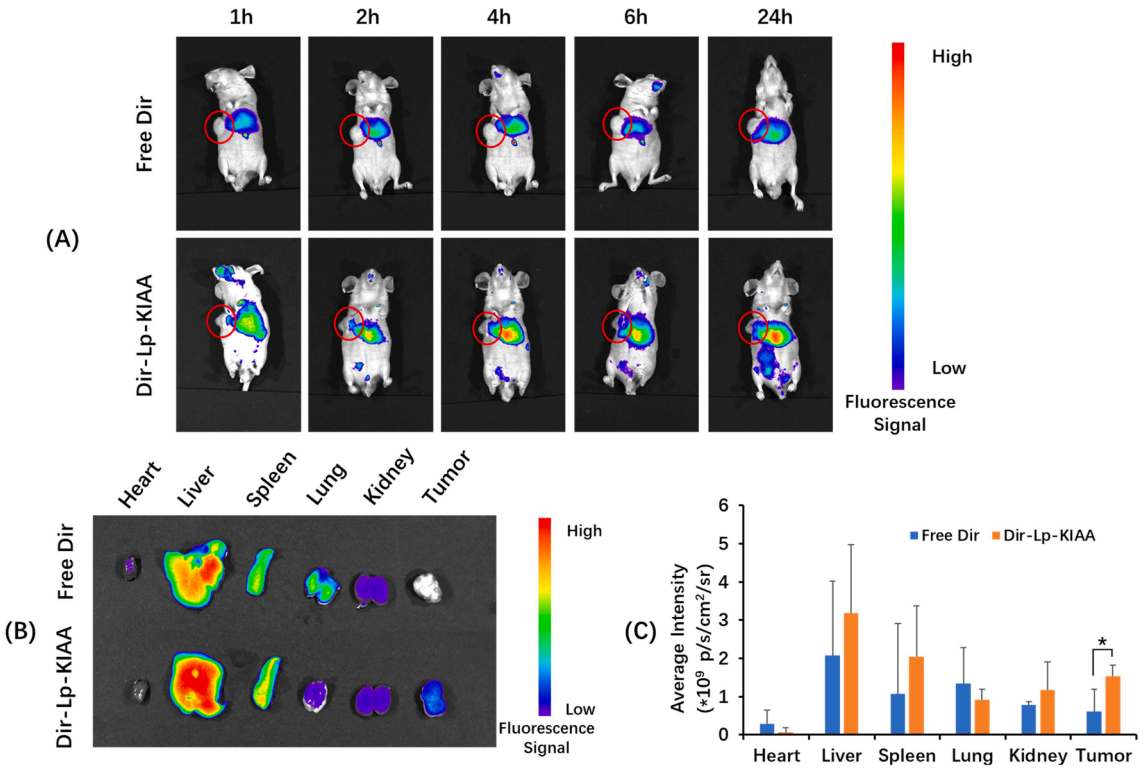

Fig. 8. Biodistribution of co-loaded liposomes in vivo. A, Representative in vivo images of mice showing the tumor distribution of Dir in HepG2 tumor-bearing mice at 1, 2, 4, 6 and 24 h. B, In vitro images of main organs and tumors. C, The corresponding average fluorescence intensity of resected tumors and major organs(means ± SD, n = 3, *P<0.05). All images of the resected tumors and major organs were included in the Supplementary Information.

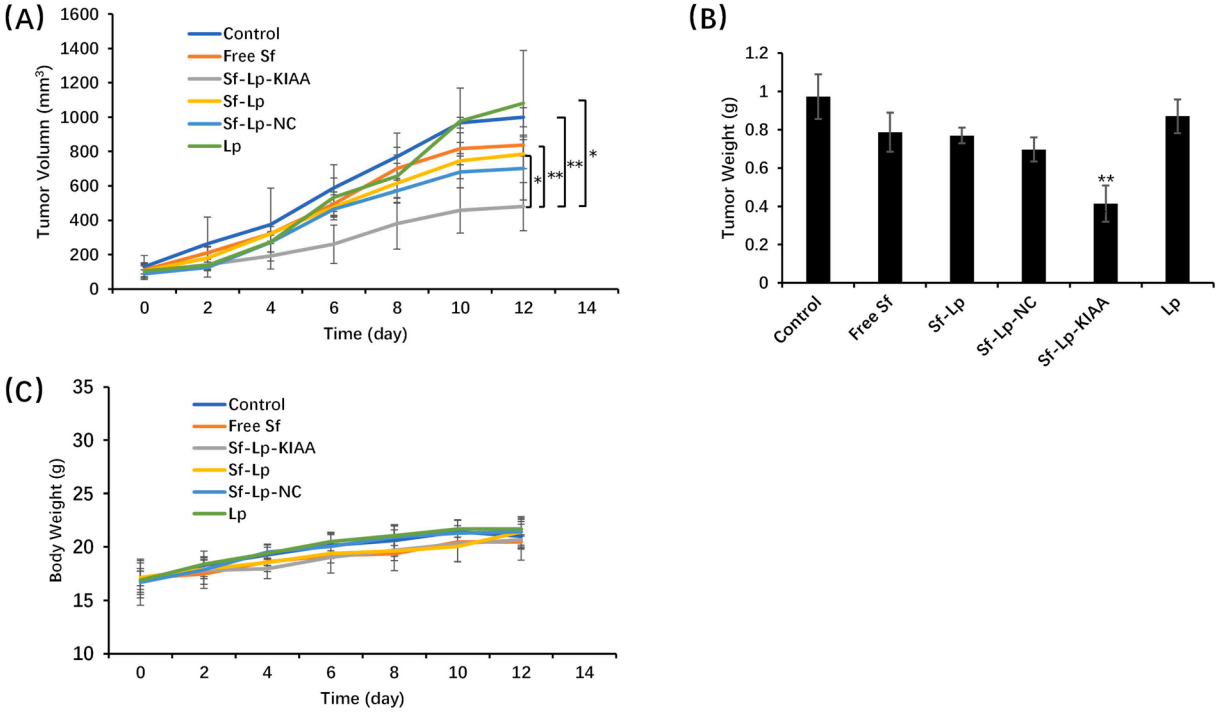

Fig. 9. In vivo anti-tumor effect. A, Tumor growth curves in nude mice treated with different formulations (means ± SD, n = 3). B, Body weight changes for the tumor-bearing mice after various formulations were given to mice on the indicated days (means ± SD, n = 3, *p < 0.05, **p < 0.01). C, Weights of the harvested tumors (means ± SD, n = 3, **p < 0.01).

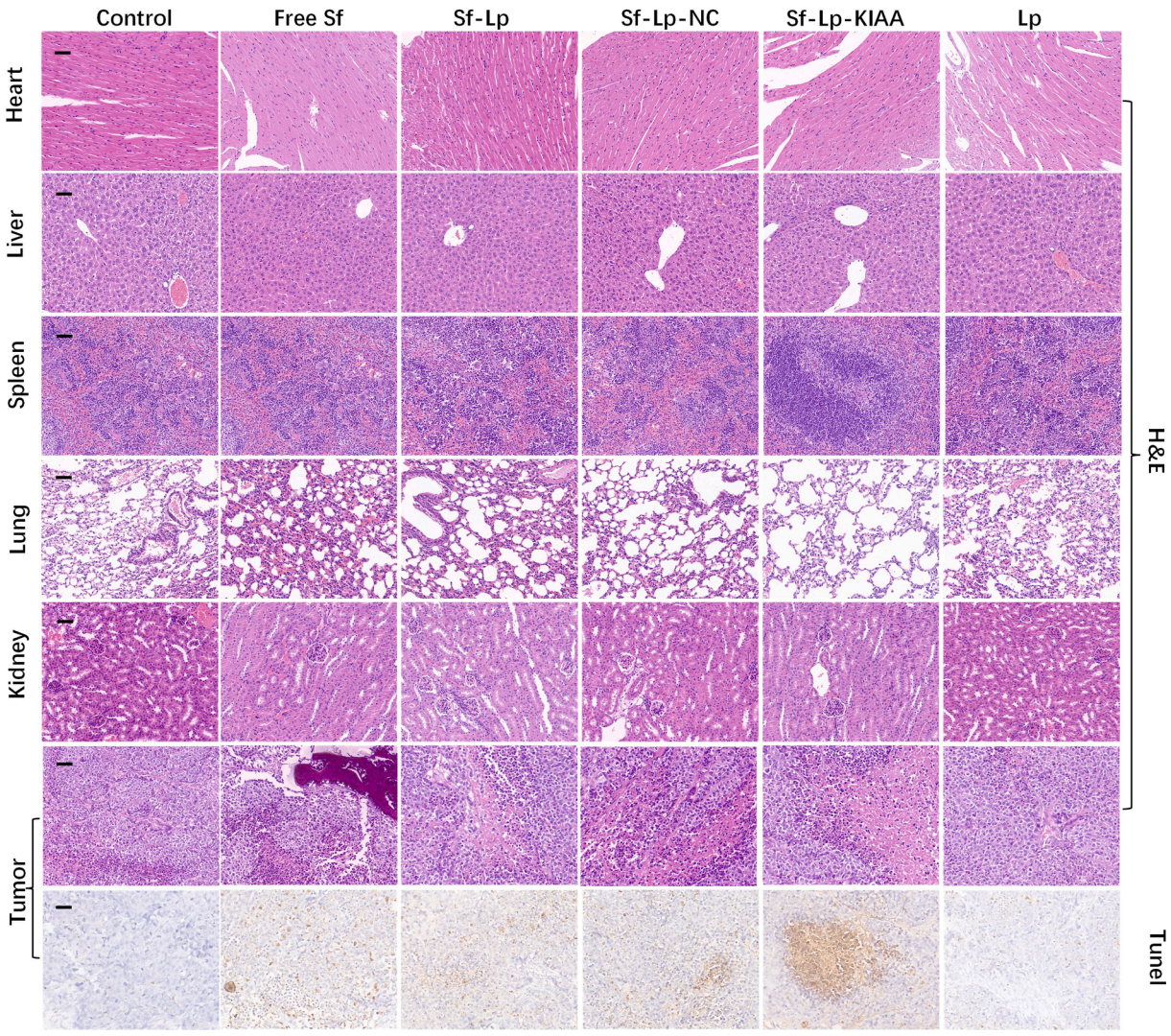

Fig. 10. Pathological analysis of the toxic side effects with H&E staining in the main organs and tumors and immunofluorescence analysis of the tumor inhibition effects with Tunel labeling. Scale bar: 50 μm.

Data curation. **Feng Xu:** Writing – review & editing, Software, Data curation. **Tingting Yao:** Writing – original draft, Funding acquisition.

Declaration of Competing Interest

The authors declare that they have no known competing financial interests or personal relationships that could have appeared to influence the work reported in this paper.

Appendix A. Supplementary data

Supplementary data to this article can be found online at https://doi.org/10.1016/j.jsps.2024.102153.

References

Ahn, J.C., Teng, P.C., Chen, P.J., Posadas, E., Tseng, H.R., Lu, S.C., Yang, J.D., 2021. Detection of Circulating Tumor Cells and Their Implications as a Biomarker for Diagnosis, Prognostication, and Therapeutic Monitoring in Hepatocellular Carcinoma. Hepatology 73 (1), 422–436. https://doi.org/10.1002/hep.31165.

Caputo, T.M., Cusano, A.M., Ruvo, M., Aliberti, A., Cusano, A., 2022. Human Serum Albumin Nanoparticles as a Carrier for On-demand Sorafenib Delivery. Curr. Pharm. Biotechnol. 23 (9), 1214–1225. https://doi.org/10.2174/1389201022666210826152311.

Cheng, Y., Ren, J., Fan, S., Wu, P., Cong, W., Lin, Y., Zhang, Q., 2022. Nanoparticulates reduce tumor cell migration through affinity interactions with extracellular migrasomes and retraction fibers. Nanoscale Horiz 7 (7), 779–789. https://doi.org/10.1039/d2nh00067a.

Chirayil, T.J., Kumar, G.S.V., 2022. Sorafenib-Entrapped, Self-Assembled Pullulan-Stearic Acid Biopolymer-Derived Drug Delivery System to PLC/PRF/5 Hepatocellular Carcinoma Model. Int J Nanomedicine 17, 5099–5116. https://doi.org/10.2147/IJN.S377354.

Desar, I.M., Mulder, S.F., Stillebroer, A.B., van Spronsen, D.J., van der Graaf, W.T., Mulders, P.F., van Herpen, C.M., 2009. The reverse side of the victory: flare up of symptoms after discontinuation of sunitinib or sorafenib in renal cell cancer patients. A report of three cases. Acta Oncol 48 (6), 927–931. https://doi.org/10.1080/02841860902974167.

Eftekhari, R.B., Maghsoudnia, N., Samimi, S., Zamzami, A., Dorkoosh, F.A., 2019. Co-Delivery Nanosystems for Cancer Treatment: A Review. Pharm Nanotechnol 7 (2), 90–112. https://doi.org/10.2174/2211738507666190321112237.

Ghaffari, M., Dehghan, G., Baradaran, B., Zarebkohan, A., Mansoori, B., Soleymani, J., Hamblin, M.R., 2020. Co-delivery of curcumin and Bcl-2 siRNA by PAMAM dendrimers for enhancement of the therapeutic efficacy in HeLa cancer cells. Colloids Surf B Biointerfaces 188, 110762. https://doi.org/10.1016/j.colsurfb.2019.110762.

Gopakumar, L., Sreeranganathan, M., Chappan, S., James, S., Gowd, G.S., Manohar, M., Koyakutty, M., 2022. Enhanced oral bioavailability and antitumor therapeutic efficacy of sorafenib administered in core-shell protein nanoparticle. Drug Deliv Transl Res 12 (11), 2824–2837. https://doi.org/10.1007/s13346-022-01142-5.

Jiang, C., Xu, R., Li, X.-X., Zhou, Y.-F., Xu, X.-Y., Yang, Y., Zheng, X.F.S., 2018. Sorafenib and Carfilzomib Synergistically Inhibit the Proliferation, Survival, and Metastasis of Hepatocellular Carcinoma. Mol. Cancer Ther. 17 (12), 2610–2621. https://doi.org/10.1158/1535-7163.Mct-17-0541.

Jiang, Z., Zhai, X., Shi, B., Luo, D., Jin, B., 2018. KIAA1199 overexpression is associated with abnormal expression of EMT markers and is a novel independent prognostic biomarker for hepatocellular carcinoma. Onco Targets Ther 11, 8341–8348. https://doi.org/10.2147/ott.S187389.

H. Kim S. Lee E. Shin K.M. Seong Y.W. Jin H. Youn B. Youn The Emerging Roles of Exosomes as EMT Regulators in Cancer Cells 9 4 2020 doi:ARTN 86110.3390/cells9040861.

Kim, J.Y., Shim, G., Choi, H.W., Park, J., Chung, S.W., Kim, S., Byun, Y., 2012. Tumor vasculature targeting following co-delivery of heparin-taurocholate conjugate and suberoylanilide hydroxamic acid using cationic nanolipoplex. Biomaterials 33 (17), 4424–4430. https://doi.org/10.1016/j.biomaterials.2012.02.066.

Koide, H., Okamoto, A., Tsuchida, H., Ando, H., Ariizumi, S., Kiyokawa, C., Oku, N., 2016. One-step encapsulation of siRNA between lipid-layers of multi-layer polycation liposomes by lipoplex freeze-thawing. J. Control. Release 228, 1–8. https://doi.org/10.1016/j.jconrel.2016.01.032.

Kong, F.H., Ye, Q.F., Miao, X.Y., Liu, X., Huang, S.Q., Xiong, L., Zhang, Z.J., 2021. Current status of sorafenib nanoparticle delivery systems in the treatment of hepatocellular carcinoma. Theranostics 11 (11), 5464–5490. https://doi.org/10.7150/thno.54822.

Li, T., Akinade, T., Zhou, J., Wang, H., Tong, Q., He, S., Leong, K.W., 2022. Therapeutic Nanocarriers Inhibit Chemotherapy-Induced Breast Cancer Metastasis. Adv Sci (weinh) 9 (33), e2203949.

Liu, Q., Zhao, K., Wang, C., Zhang, Z., Zheng, C., Zhao, Y., Liu, Y., 2019. Multistage Delivery Nanoparticle Facilitates Efficient CRISPR/dCas9 Activation and Tumor Growth Suppression In Vivo. Adv Sci (weinh) 6 (1), 1801423. https://doi.org/10.1002/advs.201801423.

Rimassa, L., Finn, R.S., Sangro, B., 2023. Combination immunotherapy for hepatocellular carcinoma. J Hepatol 79 (2), 506–515. https://doi.org/10.1016/j.jhep.2023.03.003.

Safaei, M., Khosravian, P., Kazemi Sheykhshabani, S., Mardani, G., Elahian, F., Mirzaei, S.A., 2022. Enzyme-sensitive nanoparticles, smart TAT and cetuximab conjugated immunoliposomes to overcome multidrug resistance in breast cancer cells. Toxicol Appl Pharmacol 441, 115989. https://doi.org/10.1016/j.taap.2022.115989.

Safaei, M., Khalighi, F., Behabadi, F.A., Abpeikar, Z., Goodarzi, A., Kouhpayeh, S.A., Ramezani, V., 2023. Liposomal nanocarriers containing siRNA as small molecule-based drugs to overcome cancer drug resistance. Nanomedicine 18 (24), 1745–1768. https://doi.org/10.2217/nnm-2023-0176.

Su, J.X., Li, S.J., Zhou, X.F., Zhang, Z.J., Yan, Y., Liu, S.L., Qi, Q., 2023. Chemotherapy-induced metastasis: molecular mechanisms and clinical therapies. Acta Pharmacol Sin 44 (9), 1725–1736. https://doi.org/10.1038/s41401-023-01093-8.

Tang, W., Chen, Z., Zhang, W., Cheng, Y., Zhang, B., Wu, F., Wang, X., 2020. The mechanisms of sorafenib resistance in hepatocellular carcinoma: theoretical basis and therapeutic aspects. Signal Transduct Target Ther 5 (1), 87. https://doi.org/10.1038/s41392-020-0187-x.

Wang, X., Hu, R., Song, Z., Zhao, H., Pan, Z., Feng, Y., Zhang, J., 2022. Sorafenib combined with STAT3 knockdown triggers ER stress-induced HCC apoptosis and cGAS-STING-mediated anti-tumor immunity. Cancer Lett 547, 215880. https://doi.org/10.1016/j.canlet.2022.215880.

Wang, D., Lu, S., Zhang, X., Huang, L., Zhao, H., 2020. Co-expression of KIAA1199 and hypoxia-inducible factor 1α is a biomarker for an unfavorable prognosis in hepatocellular carcinoma. Medicine (Baltimore) 99 (50), e23369.

Wang, H., Xu, L., Zhu, X., Wang, P., Chi, H., Meng, Z., 2014. Activation of phosphatidylinositol 3-kinase/Akt signaling mediates sorafenib-induced invasion and metastasis in hepatocellular carcinoma. Oncol Rep 32 (4), 1465–1472. https://doi.org/10.3892/or.2014.3352.

Woodcock, J., Griffin, J.P., Behrman, R.E., 2011. Development of novel combination therapies. N Engl J Med 364 (11), 985–987. https://doi.org/10.1056/NEJMp1101548.

Xu, J., Lin, H., Li, G., Sun, Y., Shi, L., Ma, W.L., Chang, C., 2017. Sorafenib with ASC-J9 (®) synergistically suppresses the HCC progression via altering the pSTAT3-CCL2/Bcl2 signals. Int J Cancer 140 (3), 705–717. https://doi.org/10.1002/ijc.30446.

Xu, C., Liu, W., Hu, Y., Li, W., Di, W., 2020. Bioinspired tumor-homing nanoplatform for co-delivery of paclitaxel and siRNA-E7 to HPV-related cervical malignancies for synergistic therapy. Theranostics 10 (7), 3325–3339. https://doi.org/10.7150/thno.41228.

Xu, Y., Xu, H., Li, M., Wu, H., Guo, Y., Chen, J., Li, J., 2019. KIAA1199 promotes sorafenib tolerance and the metastasis of hepatocellular carcinoma by activating the EGF/EGFR-dependent epithelial-mesenchymal transition program. Cancer Lett 454, 78–89. https://doi.org/10.1016/j.canlet.2019.03.049.

Yang, T., Li, B., Qi, S., Liu, Y., Gai, Y., Ye, P., Xu, C., 2014. Co-delivery of doxorubicin and Bmi1 siRNA by folate receptor targeted liposomes exhibits enhanced anti-tumor effects in vitro and in vivo. Theranostics 4 (11), 1096–1111. https://doi.org/10.7150/thno.9423.

Yang, C., Zhang, H., Zhang, L., Zhu, A.X., Bernards, R., Qin, W., Wang, C., 2023. Evolving therapeutic landscape of advanced hepatocellular carcinoma. Nat Rev Gastroenterol Hepatol 20 (4), 203–222. https://doi.org/10.1038/s41575-022-00704-9.

Yao, Y., Su, Z., Liang, Y., Zhang, N., 2015. pH-Sensitive carboxymethyl chitosan-modified cationic liposomes for sorafenib and siRNA co-delivery. Int J Nanomedicine 10, 6185–6197. https://doi.org/10.2147/ijn.S90524.

Ye, H., Chu, X., Cao, Z., Hu, X., Wang, Z., Li, M., Xu, L., 2021. A Novel Targeted Therapy System for Cervical Cancer: Co-Delivery System of Antisense LncRNA of MDC1 and Oxaliplatin Magnetic Thermosensitive Cationic Liposome Drug Carrier. Int J Nanomedicine 16, 1051–1066. https://doi.org/10.2147/ijn.S258316.

Yi, S., Liao, R., Zhao, W., Huang, Y., He, Y., 2022. Multifunctional co-transport carriers based on cyclodextrin assembly for cancer synergistic therapy. Theranostics 12 (6), 2560–2579. https://doi.org/10.7150/thno.70243.

Yonezawa, S., Koide, H., Asai, T., 2020. Recent advances in siRNA delivery mediated by lipid-based nanoparticles. Adv Drug Deliv Rev 154–155, 64–78. https://doi.org/10.1016/j.addr.2020.07.022.

You, A., Cao, M., Guo, Z., Zuo, B., Gao, J., Zhou, H., Zhang, T., 2016. Metformin sensitizes sorafenib to inhibit postoperative recurrence and metastasis of hepatocellular carcinoma in orthotopic mouse models. J. Hematol. Oncol. 9, 20. https://doi.org/10.1186/s13045-016-0253-6.